International Agency on Atomic Energy
SYMPOSIUM ON THE PRODUCTION OF ELECTRICAL ENERGY BY MEANS OF MHD-GENERATORS
Warsaw, 24-30 July 1968

N69-30453

SM-107/135

RESULTS OF RESEARCH ON A SINGLE-COMPONENT SYSTEM FOR A LIQUID-METAL MHD CONVERTER

by

B.G. Bogomolv, S. D. Dukhovlinov, E. V. Chernykh, and E. F. Shelkov
I.V. Kurchatov Institute of Atomic Energy
Moscow, U.S.S.R.

I. INTRODUCTION

In recent years interest in the conversion of thermal energy into electrical energy by means of liquid-metal MHD generators has grown considerably. The reason for this has been the appearance of a whole series of communications concerning the obtainment of results that promised quite alluring perspectives in the use of the liquid-metal MHD method of conversion.

Unlike other methods of energy conversion, liquid-metal MHD conversion is quite simple, which makes it actually feasible in the next few years. It offers satisfactory economic characteristics from the engineering point of view making possible temperatures that can be considered practical at the present level of development of special structural materials.

The creation of an energy installation [power plant] using the liquid-metal MHD method of conversion involves three independent, basic problems:

1. Conversion of thermal energy into flow energy of the conducting liquid (the term conducting liquid should also be understood as a two-phase flow if it has a sufficiently high electrical conductivity).

This process begins in the steam generator where heat is supplied to the working medium and ends in the thermodynamic acceleration system at the outlet [exhaust] of which the flow of the working medium has a sufficient electrical conductivity and work capacity necessary for achieving useful work in the MHD-generator duct.

2. Coversion of the flow energy of the conducting liquid into electrical energy. At high electrical conductivity of liquid metals which is approximately $10^5 - 10^6$ 1/(ohm·m) and magnetic induction in the MHD generator duct of 1-2 teslas, the velocities of the working medium lie within the limits of 20-30 m/sec. Here the hydraulic losses in the duct are quite small, the corrosion-erosion effect of the liquid metal on the structural materials is insignificant, and the MHD generator as a whole proves to be a reliable and quite efficient electrical device [machine].

3. Creation of a closed conversion flow pattern [circuit]; the solution of the problems of system startup, transient mode, as well as problems of dynamics and stability of the entire flow pattern as a whole.

The basics of plow-pattern classification suggested to date is their separation into two large groups that differ principally by the approach to the selection of the working medium. They are:

1. Single-component flow patterns where one working medium is used both in the first phase that achieves thermodynamic work in the cycle and in the liquid phase that creates a high conductivity in the MHD-generator duct.

2. Double-component flow patterns where thermodynamic work in the cycle is achieved by the vapor of one working medium and the conductivity in the generator duct is created by a second working medium in the liquid phase to which the former imparts energy of by a mixture of the two working media in the liquid phase with their subsequent separation after the MHD-generator duct.

In this report we shall examine some problems of designing the single-component MHD conversion flow pattern using potassium. The selection of a single-component flow pattern, as a first stage of operation of a liquid-metal MHD converter, is basically determined by the simplicity of the flow pattern and the reality of the processes included in it.

The principal flow pattern of a single-component plant having a liquid-metal MHD generator to be examined is shown in figure 1.

The cycle of the MHD plant with condensation of the vapor using a cooled liquid is schematically drawn in T - S coordinates in figure 2.

Here:
- 0-1 The vaporization of the liquid in the steam generator
- 1-2' The theoretical expansion process in the two-phase nozzle
- 1-2 The actual expansion process in the two-phase nozzle
- 2-3 The condensation process in the mixing chamber (it is understood that $P_{mc} = const$; $T_{mc} = const.$).
- 3-4' The theoretical compression process in the diffusor [exit cone]
- 3-4 The actual compression process in the diffusor
- 4-5' The theoretical energy conversion process in the MHD-gen. duct
- 4-5 The actual energy conversion process in the MHD-generator duct
- 5-6' The theoretical process in the auxiliary MHD-generator duct
- 5-6 The actual process in the auxiliary MHD-generator duct
- 5-7 The liquid-cooling process in the condensor
- 7-8' The theoretical liquid-acceleration process in the liquid nozzle
- 7-8 The actual liquid-acceleration process in the liquid nozzle
- 6-0 The process of heating the liquid in the steam gen. to boiling

It is convenient to perform the analysis of the thermodynamic cycle in dimensionless paramaters as

$$\alpha = \frac{r_1 x_1}{C_1 T_1};\quad \tau = \frac{T_2}{T_1};\quad \mu = \frac{G_{liq}}{G_{vap}};\quad H = \frac{W_{liq}}{W_{vap}};\quad \eta_{dif};\ \eta_{liqn};\ \eta_{vapn};\ \eta_{MHDg}$$

The thermal efficiency of the cycle can be written in dimensionless parameters as

$$\eta_t = \frac{H_{1-2}}{Q} = \frac{(1-\tau)(1+\alpha)-\tau\ \ln\ (1/\tau)}{1-\tau+\alpha} \qquad (1)$$

Then the internal efficiency of the cycle, equal to the ratio of the available energy to the introduced heat, is written (2)

$$\eta_i = \eta_t\cdot\eta_{acc}\cdot\eta_{vapn} = \frac{(1-\tau)(1+\alpha)-\tau\ \ln\ (1/\tau)}{1-\tau+\alpha}\cdot\frac{(1+\mu H)^2\cdot\eta_{dif}\cdot\eta_{liqn}-\mu H^2(1+\mu)}{(1+\mu)\cdot\eta_{liqn}}\cdot\eta_{vapn}$$

By examining the value of the efficiency of the acceleration device η_{acc} (second fraction in formula 2), it is possible to come to the conclusion that the optimum value of the relative wake velocity $H = H_{opt}$ must exist at which the efficiency of the acceleration device reaches a maximum:

$$H_{opt} = \frac{\eta_{dif}\cdot\eta_{liqn}}{1+\mu(1-\eta_{dif}\cdot\eta_{liqn})} \qquad (3)$$

The analysis of the dependence (2) shows that at a deviation of H from the optimum value by 20-30 per cent, the lowering of the internal efficiency of the cycle is small and consists only of 3-5 per cent.

The relative efficiency of the acceleration device $\overline{\eta}_{acc} = \frac{\eta_{acc}}{\eta_{acc}^{max}}$ as a function of the value $\overline{H} = \frac{H}{H_{opt}}$ at different values of the injection coefficient μ is shown in figure 3.

The optimum dimensionless dryness of the vapor defined from the conditions of maxium internal efficiency of the cycle can be written as"

$$\alpha^{opt} = -\frac{1-\tau}{1+\tau} + \left[\tau\frac{1-\tau}{1+\tau}\left(\frac{1-\tau}{1+\tau} + \frac{\delta_{liq}}{1-\eta_{dif}\eta_{liqn}}\right)\right]^{\frac{1}{2}} \qquad (4)$$

The transition from the optimum degree of dryness α^{opt} to the value α as a function of the ratio of the temperature of the cycle τ and the complex $\frac{\delta_{liq}}{1-\eta_{dif}\eta_{liqn}}$ is shown in figure 4.

One of the ways of increasing the internal efficiency is the introduction of the regeneration of heat in the cycle. The internal efficiency of a cycle with regeneration is expressed similar to the internal efficiency of a simple cycle and can be written in the form:

$$\eta_i = \eta_t\cdot\eta_{acc}\cdot\eta_{vapn} = \frac{\alpha(1-\tau)+\beta-\tau\ \ln(1+[\beta/\tau])}{\alpha+\beta}\cdot\frac{\eta_{dif}}{1+\frac{\alpha+\ln(1+[\beta/\tau])}{1-\tau_{liq}}(4\eta_{dif}\eta_{liqn})}\cdot\eta$$

?

The analysis of the cycle with regeneration shows that the optimum internal efficiency of the cycle can reach values of $\eta_i = 0.1\text{-}0.12$, which exceeds the value of the internal efficiency of a simply cycle by a factor of 1.3-1.4. One should also note that the regeneration of heat leads to an increase in the flow rates of the working medium and a decrease in velocities, which is substantial for small power plants where the scaling factor strongly affects the effectiveness of the elements of the system.

II. INVESTIGATIONS OF A SYSTEM OF THERMODYNAMIC ACCELERATION AND OF ITS BASIC ELEMENTS

The effectiveness of the MHD conversion flow pattern along with the achievement of a thermodynamic cycle is defined by the achievement of each element of the pattern. Since the basic difficulties of creating a single-component plant with a liquid-metal MHD generator are included in the development of an effective system of thermodynamic acceleration of the working medium, interest in testing complex [sophisticated] models of accelerating devices and their basic elements [components] is completely understandable.

Thermodynamic work in the cycle is achieved by moist steam [vapor] in the two-phase nozzle. The physical pattern of the process in the single-component vapor-liquid nozzle is extremely complex. Unlike the single-phase flow, here the effects on the vapor phase in the course of its expansion must conflict with several factors. In this case geometric reaction and mass reaction take place as a result of the vaporization of the liquid phase. Furthermore, the vapor achieves the work through aerodynamic acceleration of the drops suspended in it. Since the thermodynamic process in this type of nozzle strongly differs from the isentrope, one should take into consideration the effect of heat. It is not possible to give a precise analytic solution of this type of flow [ref. #1].

Therefore, a semi-empirical method of calculating the two-phase nozzle has been suggested. As the experiment shows [ref. #2], the expansion process is thermodynamically stable. The flow is regarded as unidemensional. Having separated a section of the length element into an arbitrary cross section of the nozzle dl where change elements of pressure dp occur, and the masses and velocities of the liquid and vapor phases obtain conversion elements dm_{liq}, dW_{liq}, dm_{vap}, dW_{vap}, the change in the momentum of the mixture is examined in this section. Here it is understood that the forces of external pressures and resistance of the drops moving in it are acting on the vapor portion of the current [flow], and the force of friction against the walls of the nozzle on the mixture:

$$dF_{fr} = SK_{fr} \frac{dl}{D_n} \rho_{mix} \frac{W^2_{mix}}{2}$$

As a result, we obtain an expression for the determination of the local efficiency which, for the case $x \gg \frac{\rho_{vap}}{\rho_{liq}} \frac{(1-x)^2}{\bar{W} - x}$, when it is possible to put $\rho_{mix} \approx \frac{\rho_{vap}}{x}$, has the form:

$$\eta = \frac{dE_{mix}}{dE_{meas}} = \frac{\bar{W}}{1+\Omega\bar{W}\left(\frac{\bar{W}-x}{1-\bar{W}}\right)^2} \tag{5}$$

here $W = x+(1-x)\frac{Wliq}{Wvap}$ is a dimensionless parameter that takes into consideration the variety of velocities of the vapor and liquid phases, $\Omega = \frac{4}{3}\frac{K_{fr}}{C_x}\frac{r_d}{D_n}\frac{\rho liq}{\rho vap}$ is a dimensionless local complex that characterizes the effectiveness of acceleration of the liquid phase of the two-phase nozzle (the criterion of acceleration). The expression for determining the length of the nozzle is

$$dl = \Omega\frac{D_n}{K_{fr}}\left(\frac{\bar{W}-x}{1-\bar{W}}\right)^2\frac{dE_{mix}}{E_{mix}} \tag{6}$$

The analysis of the obtained dependences indicate the following: the parameter $\bar{W}$ is always greater than x and less than 1. The case $W = 1$ corresponds to a nozzle of infinite length. The case $W \to x$ corresponds to the absence of mechanical interaction of the phases, i.e., a nozzle of zero length. Expression (5) shows that the decrease of K, η_d, ρ_d as well as the increase of C_x, D_n, ρ_{vap} leads to an increase in the efficiency of the nozzle. Thus, the criterion of acceleration qualitatively reflects the influence of the geometric and mode parameters of the current, the quality of the surface of the flow portion, and the properties of the working medium.

From expression (5) it can be easily noted that in each cross section of the nozzle there is an optimum local value of the parameter that corresponds to the maximum efficiency of the nozzle and for the case $x \ll 1$ and $x \ll \bar{W}$, $\bar{W}_{opt} = \frac{1}{1+(2\Omega)^{1/3}}$. Furthermore, from expressions (5) and (6) it is clear that the presence of friction against the walls of the nozzle slightly affects the length of the nozzle, while the efficiency essentially depends on the value of the coefficient of friction. In order to integrate the above written expressions, it is necessary to know the law of distribution of the drops according to [their] dimensions, the coefficient of resistance of the vaporized drops along the vapor flow, and the mechanism of interaction of the drop current [flow] with the wall of the nozzle. The scope of these problems has been slightly investigated. In order to calculate the nozzles, the following assumptions are understood: The size of the drops is formed at the critical size and with a cross section close to it, and remains constant along the length of the nozzle, here the radius of the drops is determined by Weber's criterion understood [taken] to be equal to 6, the coefficient of resistance of the drops is determined [defined] as the coefficient of resistance of a sphere in the gas flow.

Figure 5 presents the efficiency of the two phases of the nozzle as a function of its length; this dependence is calculated and experimentally obtained by purging [blowing through] series of three nozzles of different lengths.

Figure 6 shows a change in the efficiency of the nozzle as a function of the changes in the operating factors. Here a nozzle of optimum length was investigated at constant counterpressure and varied pressure of the vapor at the inlet into the nozzle.

The measured values of the efficiency of the nozzles are close to nominal considering the forces of friction to be K_{fr} = 0.03. The efficiency maximum is reached at a length of 120 mm and consists of η = 0.45.

Thus, the single-component two-phase nozzles can be calculated according to the method discussed. The experimental verification of the method, which showed satisfactory agreements of the theory with the test, confirms the accuracy of the theoretical approach to the solution of the problems.

MIXING CHAMBER, DIFFUSOR WITH CONDENSATION JUMP

In the initial stage of work on the study of condensation processes of high velocity vapor flows using a supercooled liquid, basic attention was directed to the appearance of the physical pattern of the processes. Different methods of feeding [supplying] the liquid were tested: in the form of a ring film, peripheral jets, and central monojets. The best results were obtained with a monojet and further work was performed with this type of model. Water was used as the working medium.

In order to investigate the operation of the mixing chamber—the term mixing chamber is understood as a part of the thermodynamic acceleration system, where the combining of the vapor and liquid flows are combined and the former is condensed, the operation of all systems is necessary. The selected design of the acceleration device, as we shall call the system of thermodynamic acceleration of the working medium, made it possible to set [up] various mixing chambers with a constant geometry of the vapor nozzle. Observations were made by sampling the flows as to pressure and temperature, visually, by arranging experimental sections of glass, by photographing external characteristics, by oscillographic recording of pressure pulsations in various parts of the models under study.

On the basis of the investigations performed, there now exists the following concept of the condensation process of moist vapor flow in the liquid jet.

Actually, condensation proceeds along the surface of the jet and heat is transmitted to the main mass of the cooling liquid by turbulent mixing. The speed of this type of heat-transfer mechanism is shown in the paper [ref. #4]. However, the structure of the jet varies along its length. Thus, in the initial [or: front] cross sections, for example, of 2 caliber [bore gauge], purely liquid [cross] section take place, furthermore, penetration begins into the main mass of the liquid of the vapor-gas occulsions, which reaches saturation at some length on the order of 20 caliber and which is characterized by the relative density of approximately 0.5; further increase in the length of the jet has no essential effect. In the tests, the length of the jet varied from 3 to 40 caliber. The jet reaches the entrance to the diffusor [exit cone] in the form of a frothy liquid. Flows that have this type of structure are not stable in the flow in ducts and abruptly change into the liquid phase that contains residue of non-condensed gases dissolved in the main mass of the liquid for lengths of time that considerably exceed the collapse time of each individual bubble in the jump. The position of the jump zone is defined by the counter-pressure that is created at the outlet of the acceleration device. At the highest counterpressure, the jump zone is located in the entrance to the diffusor and in its expansion section. When the counterpressure decreases, there is a shift of this zone into the expansion section. Pressure pulsations in the jump are caused by the fact that the characteristic velocity of collapse of the bubbles is greater than the flow velocity at the inlet into the jump zone.

Figures 6 and 7 show a photograph of the flow in the mixing chamber at the greatest counterpressure with the pressure distribution along the length and an oscillogram of the jump.

ACCELERATION DEVICE

Parallel with the study of condensation processes, work was conducted on the investigation of the acceleration device as a whole, i.e., on locating the limiting operating conditions, on the effect of vapor parameters at the inlet, etc.

The work was performed on a [test] stand having a single-tube steam generator with 100-KW electrical heating. The pump produced a pressure up to 12 atm at the outlet. Flow rates were measured in the vapor and liquid loop of the circuit, pressures and temperatures at the inlet and outlet of the acceleration device, in the mixing chamber, [and] steam-generator power.

It is shown experimentally that the system is capable of work at any vapor dryness at the inlet into the vapor nozzle. However, work with vapor having a dryness of 0-0.05 is connected with strong pulsations of pressure and flow rate caused by the implemental [?] mode of the steam generation. "Quiet" operation with the liquid in the vapor loop of the circuit is fundamentally possible, operation which reaches the parameters of saturation in the throat of the vapor nozzle, the so-called boiling nozzle. Pulsationless operation in this case is caused by localization of the beginning of boiling in the throat of the vapor nozzle.

The effect of the injection speed [velocity] of the cooling liquid at the inlet into the mixing chamber, with constant flow rate, was explained by means of a change in the outlet cross section of the nozzle. It is shown that the change in the injection speed does not cause any appreciable effect on the operation of the vapor nozzle. With the decrease in the injection speed, the maximum pressure at the outlet of the acceleration device is somewhat lower. An increase in the area of shear of the liquid nozzle above the area of the diffusor throat introduces no limits to the operation of the acceleration device. In other experiments the area of shear of the liquid nozzle exceeded the throat of the diffusor by a factor of 4. Boundary values of the flow rate of the cooling liquid were obtained at constant parameters of the vapor at the inlet. At the smallest flow rate there is a cutoff of the operation of the vapor nozzle, at the greatest, there is a blocking of the flow at the outlet of the mixing chamber. One should note the dependence of the boundary values on the injection speed, the boundary values of the flow rate were 0.47 and 1.52 of the nominal flow rate, with a decrease in injection speed to 0.7 of the nominal 0.68 and 1.38 respectively, to 0.5 of the nominal 0.78 and 1.26, and to 0.4 of the nominal 0.85 and 1.2.

Fiugre 8 shows one of the external characteristics taken at constant flow rate and vapor dryness. The excess of the outlet temperature of the liquid form the acceleration device above the vapor temperature in the mixing chamber at small coolant flow rates is explained by the fact that a non-isobaric mixing chamber was used in this model, i.e., the pressure increased along its length. Pressure and temperature were measured in the initial section of the mixing chamber. Let us not incidentally that in all tests with the exception of operation of the boiling nozzle, a thermodynamic state of non-equilibrium, i.e., the divergence of the temperature or pressure from the equilibrium curve, was not noted in the flows of moist vapor. In order to explain the operation of the acceleration device as a function of the vapor pressure at the inlet, a number of blow-throughs [purges] were made on the model itself [the same model]. The change in vapor pressure at the inlet was obtained by changing the flow rate and the power of the steam generator. The generalized characteristics are shown in figure 9. From the graph it is evident that with the increase of the vapor pressure, the derivative $\frac{dp_{out}}{dp_{liq\ in}} / p_{vap}$ rises with the increase of the vapor pressure . This result diverges from data presented in [ref. #5]. Possibly this is caused by a scale effect [or: the effect of scale]. The level of the power of the plant at which the experiments presented in this paper were performed exceeds the power of our test stand by more than one order of magnitude.

III. CLOSED FLOW PATTERN

The obtained level of pressures at the outlet of the acceleration device made it possible to go to the closed system of thermodynamic acceleration of the working medium with the production of the useful work. Problems of the controllability and the stability of these systems operating in various modes are to solved experimentally.

Startup takes placy by means of an actuating pump. After the steam generator reaches the nominal parameters and the acceleration device starts up, we change the flow pattern to a self-pumping mode by opening the valves of the bypass line of the pump and simultaneously close the valves cutting off the pump. The useful work is reduced by a throttle at the outlet of the acceleration device and imitates a generator.

It is shown experimentally that this system is easily controlled and has automatic stability, if the vapor dryness at the outlet of the steam generator is not less than 0.05. Operation with lower degrees of dryness, as indicated above, is associated with strong pulsations that can lead to spontaneous cutoff. Operation with the acceleration device that uses the boiling nozzle is characterized by the clearly expressed instability caused by strong dependence of the equilibrium pressure on the temperature. The insignificant increase in the liquid temperature at the outlet of the steam generator (in this case of the heater) leads to an increase in pressure, which leads to blocking of the flow rate in the vapor loop with constant pressure at the inlet, and in the opposite case to the increase in the flow rate and cutoff of the acceleration device operation. Stable operation with moist vapor is explained by the fact that a similar pattern, with small changes in the flow rate, brings a slight increase (decrease) of steam generator power to a rise (drop) in pressure in the expansion tank, thanks to the change in the volume of the vapor, which leads to a change in the flow rate, bringing the system into equilibrium.

The different pressures at the outlet of the acceleration device prior to its boundary value do not affect the operation [work] of the flow pattern. The load characteristics of the acceleration device are similar to the characteristics of volume engines. This property produces a series of requirements on the generator to assure its stable operation in a flow pattern [circuit] together with the acceleration device.

As has already been stated, the expansion tank fulfills the role of a system regulator, i.e., the level of pressure in it must determine the stability of the flow pattern. A number of data are presented:

Volume of circuit	50 liters
Vapor pressure at inlet into the nozzle	2 atm
Vapor dryness at the inlet into the nozzle	0.1
Pressure at the inlet to teh liquid nozzle	2.5 atm
Pressure at the outlet	8 atm
Volume of gas in the expansion tank	5 liters, 10 l, 15 l
Smallest pressure in expansion tank at which the flow pattern is stable	3.4 atm, 3.5 atm, 3.6 atm

It is obvious that with an increase of the gas volume in the expansion tank, the pressure in it can still decrease, but this must involve with it a change in the filling of the circuit with a working medium in the startup process, which is probably not technically justified, since the pressure consumed in control, 1-2 atm, is comparatively small.

Figure 10 shows an oscillogram of pressure in various sections of the circuit in a pulsating system. Pulsations are caused by a decrease of pressure in the expansion tank below the critical. Pulsations of the flow rate in the vapor loop considerably exceed the pulsations in the liquid loop. The amplitude of the flow-rate pulsations in the vapor loop in the mode shown in figure 10 were 30 per cent of its nominal value. As is seen from the oscillograms, the pressure varies insignificantly at the outlet of the steam generator with this strong change in the flow rate.

In another series of experiments, the effect of the change in the power fed to the steam generator on the operation of the flow pattern was explained. For technical reasons a 20-percent change in power from the nominal occurred in ~5 sec. Figure 11 shows an oscillogram with the 20-percent increase in power, and figure 12 an oscillogram with a 20-percent decrease in power.

In all the oscillograms presented, the speed of film movement is 10 mm/sec.

Tail I Vapor pressure at inlet to the acceleration device

Tail II Liquid pressure at inlet to the acceleration device

Tail III Pressure in expansion tank

Tail IV Pressure in jump zone

Tail V Pressure at outlet of acceleration device

As is seen from the oscillograms, the introduced disturbance in power is most strongly expressed just at the position of the jump, the disturbance being characterized by the pressure at the control [reference] point, tail IV. As the power of the jumps rises, it goes off into the region of larger cross sections, the so-called flow energy [power] grows, which leads to a drop in the pressure at the reference point, and conversely.

The step-by-step change of the flow rates in the vapor and liquid loop of the circuit by 10 per cent of the nominal value leads to a smooth transition of the system to a new operating point. No fluctuations of any of the parameters were noted in any of the experiments.

Tests conducted to determine the level of stability of the examined closed system of thermodynamic acceleration of the working medium make it possible to confirm that no problems of stability and of controllability will arise with these systems.

IV. CONCLUSION

Work performed in the investigation of the system of thermodynamic acceleration and its elements shows that the fundamental processes based on it are physically real, made it possible to record [note] tangible ways to further increase the effectiveness of the entire system.

References

1. Nakhman, Yu.V., *Equations for the Analysis of the Flow of Moist Vapor*, Izvestiya VUZ Energetika, No.9, 1963.

2. Polozhiy, S.V., *Experimental Investigations of the Adiabatic Vapor Conversion while Flowing in a Nozzle*, Izvestiya VUZ Energetika, No.9, 1963.

3. Vaysman, M.D., *The Thermodynamics of Liquid Vapor Streams*, 1967.

4. Dukhovlinov, S.D., *Condensation of Vapor Wake in a Liquid Stream*, Teplofizika Vysokykh Temperatur, No.3, 1967.

5. Brow, G.A. and Levy, E.K., *Liquid Metal Magnetohydrodynamic Power Generation with Condensing Ejector Cycles*, Proceedings of a symposium on MHD Electrical Power Generation, Salzburg, July 1966.

Nomenclature

ρ	Density
r	Heat of Vapor Conversion
C	Heat capacity
T	Temperature
p	Pressure
H	Enthalpy
G	Specific heat
G_{liq}	Mass flow of liquid
$G_{\ddot{\pi}}$	Mass flow of vapor
D	Diameter of the cross section of the nozzle
r_d	Radius of a drop
x	Degree of vapor dryness
C_x	Coefficient of resistance
K_{fr}	Coefficient of friction
T	Dimensionless temperature
μ	Coefficient of injection
$\varkappa$	Relative velocity
a	Dimensionless thermophysical complex
p	Dimensionless thermal pressure in the generative nozzle
η_{dif}, $\eta_{liq\ n}$, $\eta_{vap\ n}$, $\eta_{MHD\ G}$, η_{acc}	Coefficient of complete diffusor action, liquid nozzle, vapor nozzle, MHD generator, accelerator
inl	Parameters at the accelerator intake
m.c.	Parameters in the mixing chamber
outl	Parameters in the accelerator outlet
Vap	Vapor
liq	Liquid
Mix	Mixture

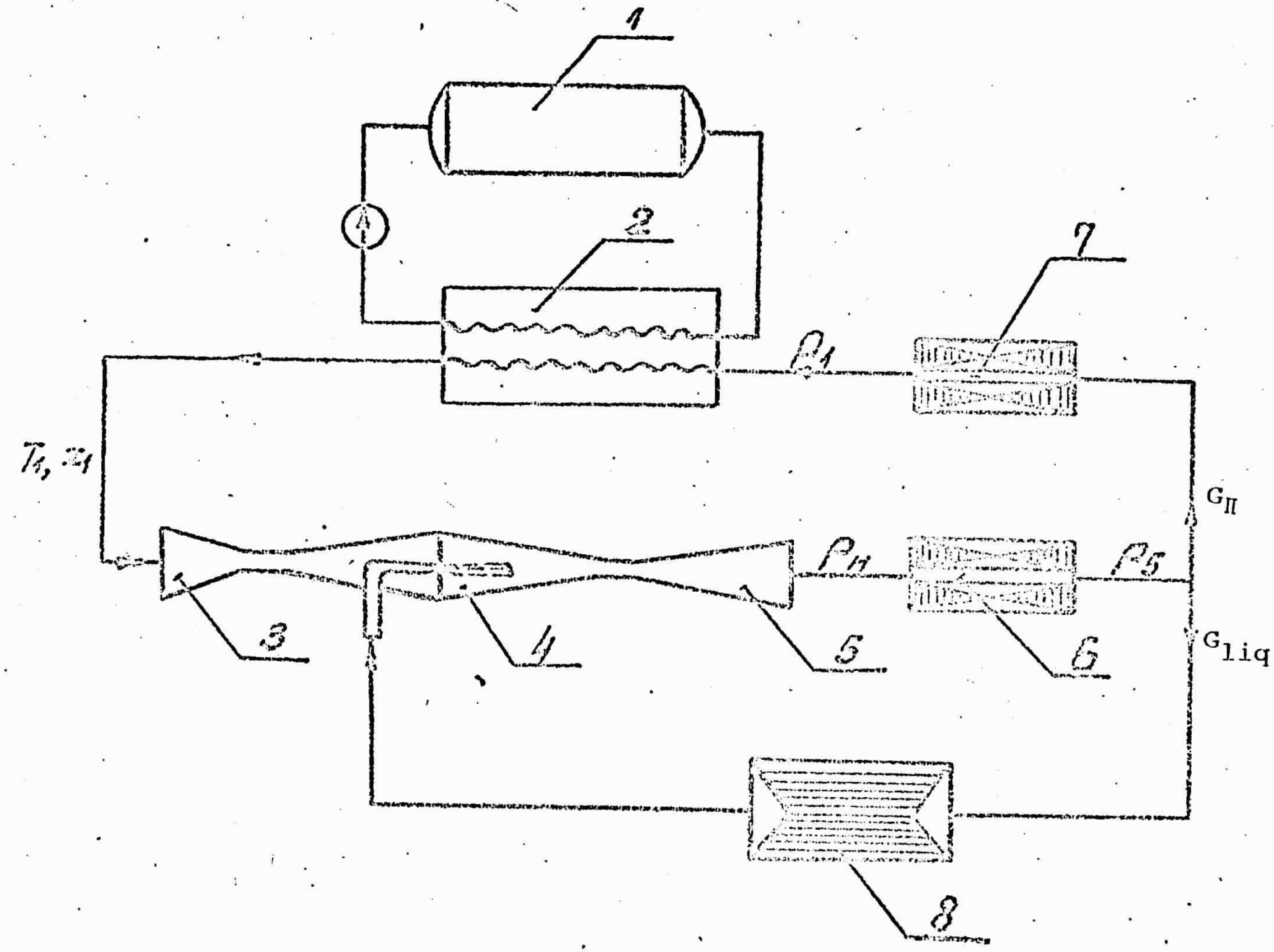

Фиг.1 Принципиальная схема системы с ж.м. МГД-генератором

Fig. 1. Main schematic of an MHD generator with a liquid-metal system.

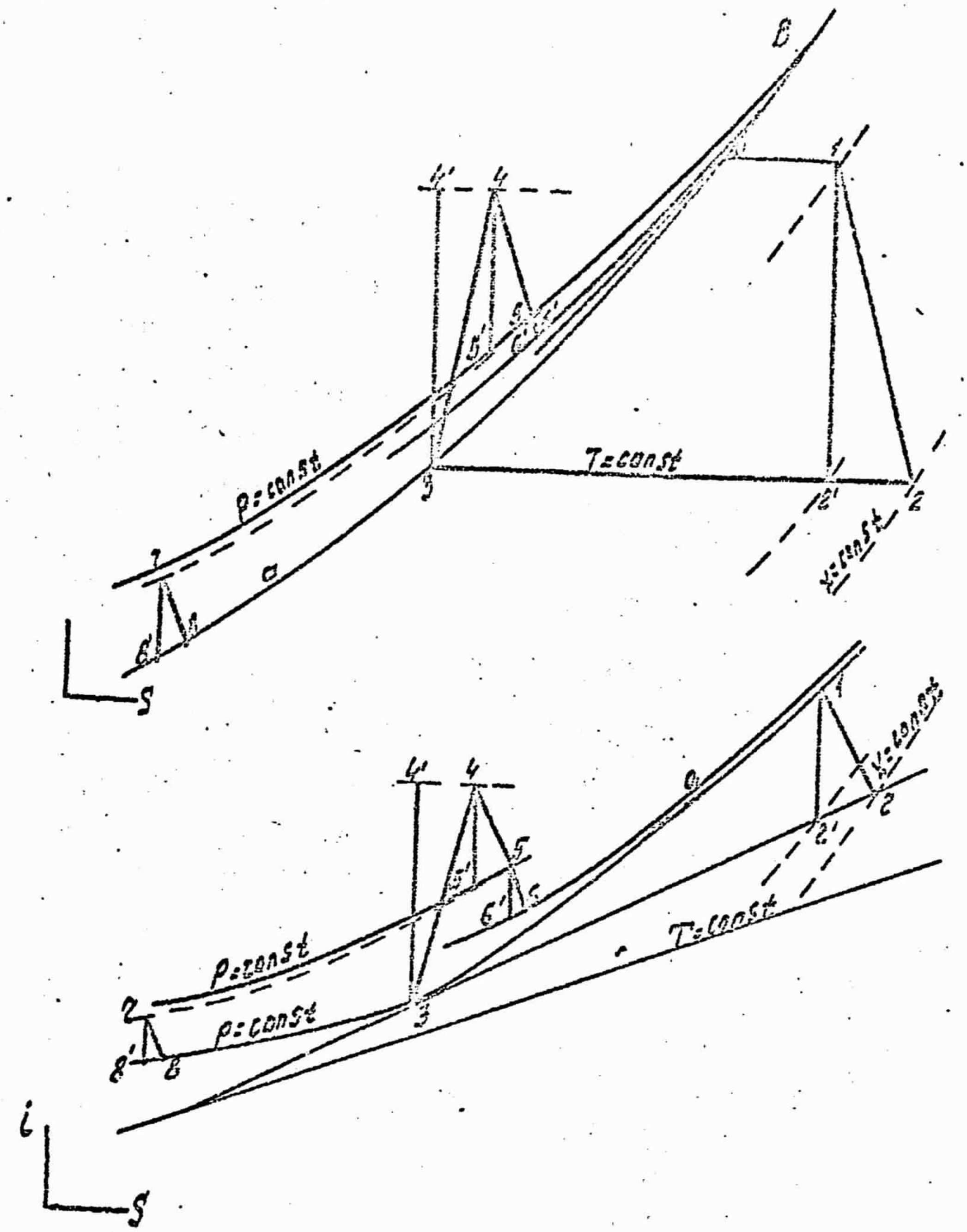

Фиг. 2

Схематическое изображение цикла в T-S и I-S координатах

Fig. 2. Schematic presentation of a cycle in T - S and I - S coordinates.

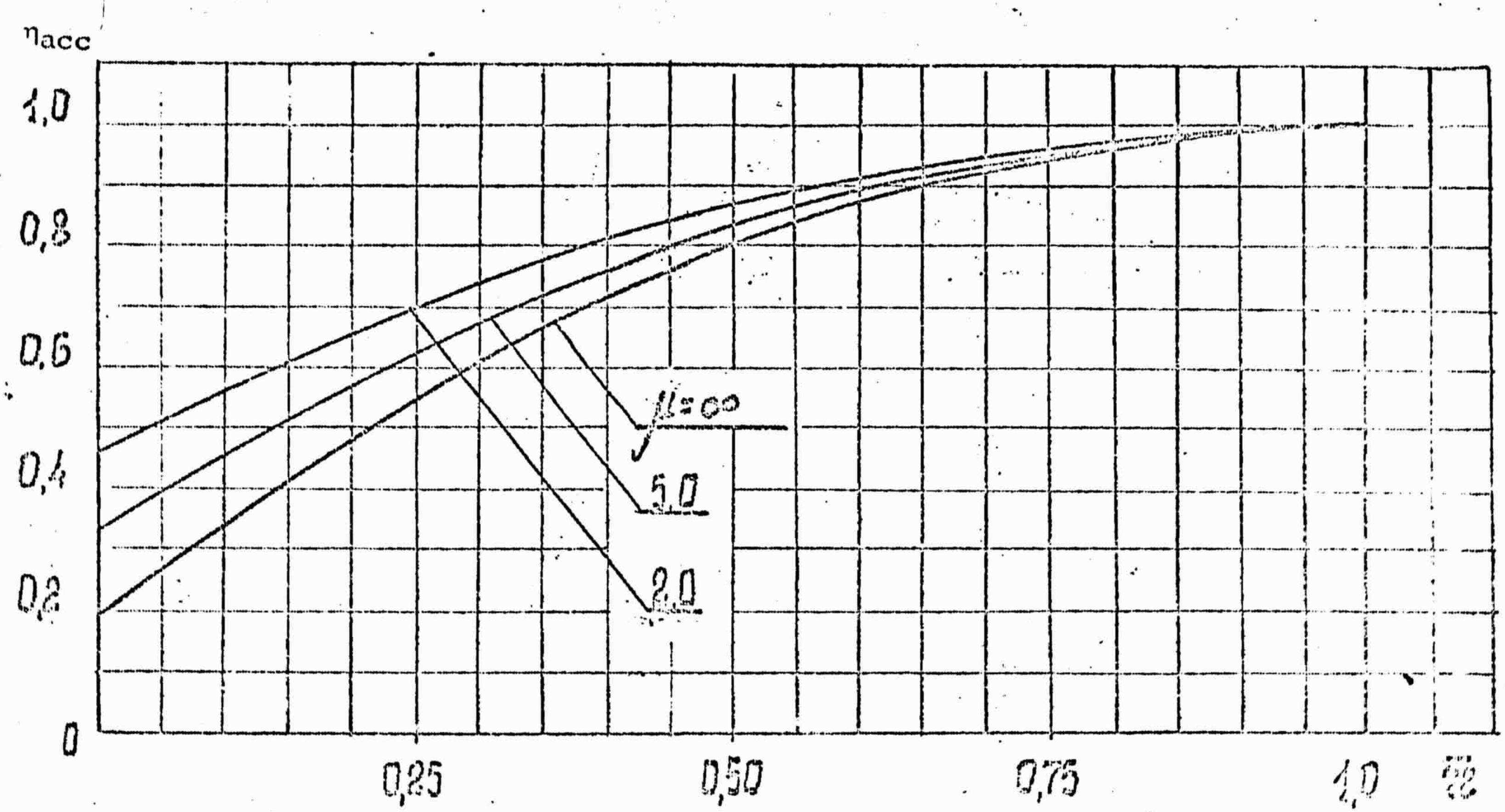

ФИГ. 3. ЗАВИСИМОСТЬ КПД РАЗГОННОГО УСТРОЙСТВА $\bar{\eta}_{ру} = \frac{\eta_{ру}}{\eta_{ру\,max}}$ ОТ ОТНОСИТЕЛЬНОЙ СПУТНОЙ СКОРОСТИ $\bar{\vartheta} = \frac{\vartheta}{\vartheta_{опт}}$ И КОЭФФИЦИЕНТА ИНЖЕКЦИИ μ.

Fig. 3. Dependence of efficiency of the accelerator $\eta_{acc}{}^{2} = \eta_{acc}/\eta_{acc\ max}$ on the relative velocity $= \varkappa/\varkappa_{opt}$.

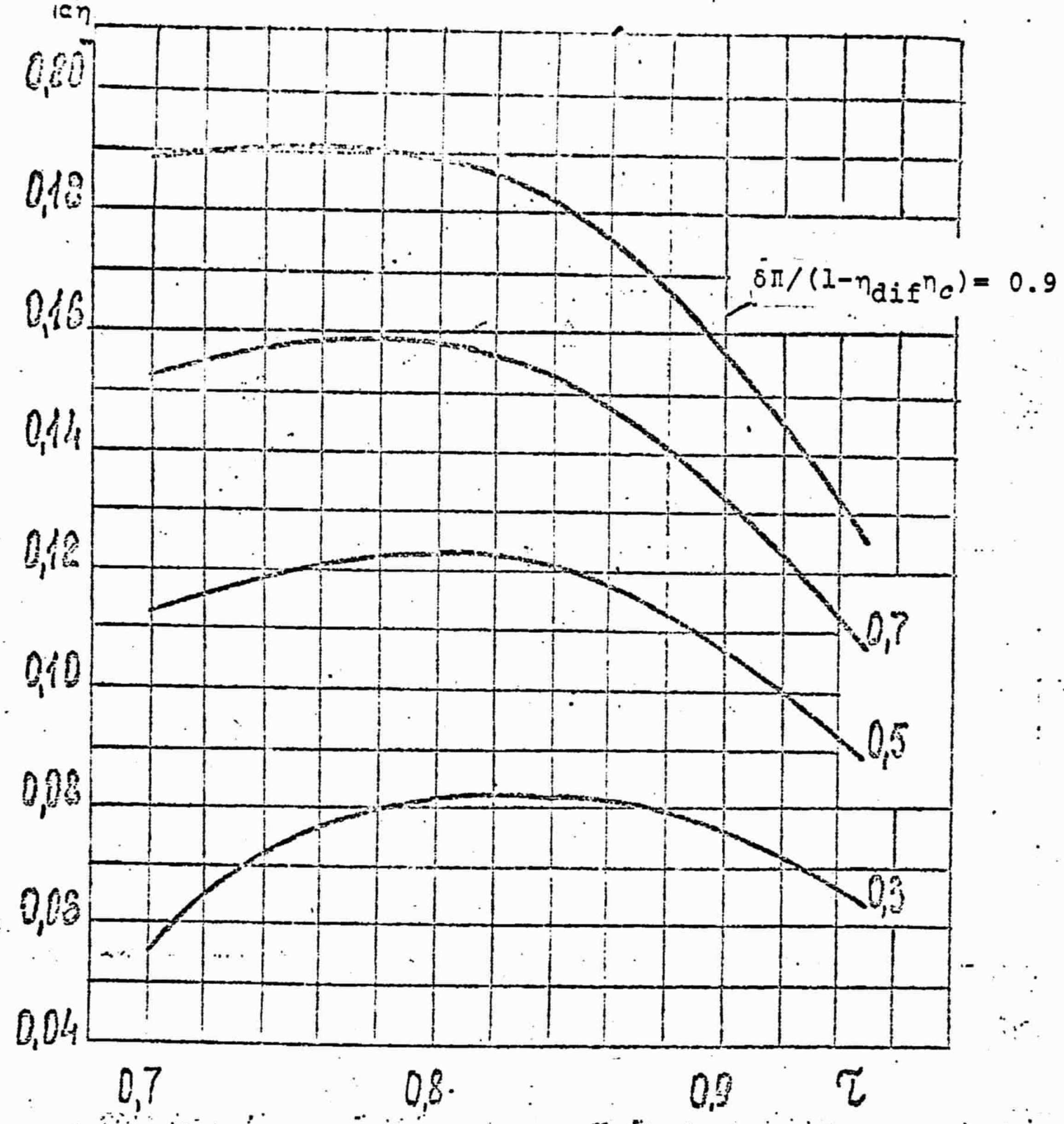

ФИГ. 4. ЗАВИСИМОСТЬ ОПТИМАЛЬНОГО ПО КПД ЗНАЧЕНИЯ ПАРАМЕТРА $\alpha_2 = \frac{r_1 x_1}{c_1 T_1}$ ОТ ОТНОШЕНИЯ ТЕМПЕРАТУР $\tau = \frac{T_3}{T_1}$ И ПАРАМЕТРА $\frac{\delta_\pi}{1-\eta_d \eta_c}$.

Fig. 4. Dependence of an optimal efficiency value of the parameter $\alpha_2=r_1x_1/c_1T_1$ on the relation of temperature and the parameter .

NOTE: Blank spaces represent illegible text.

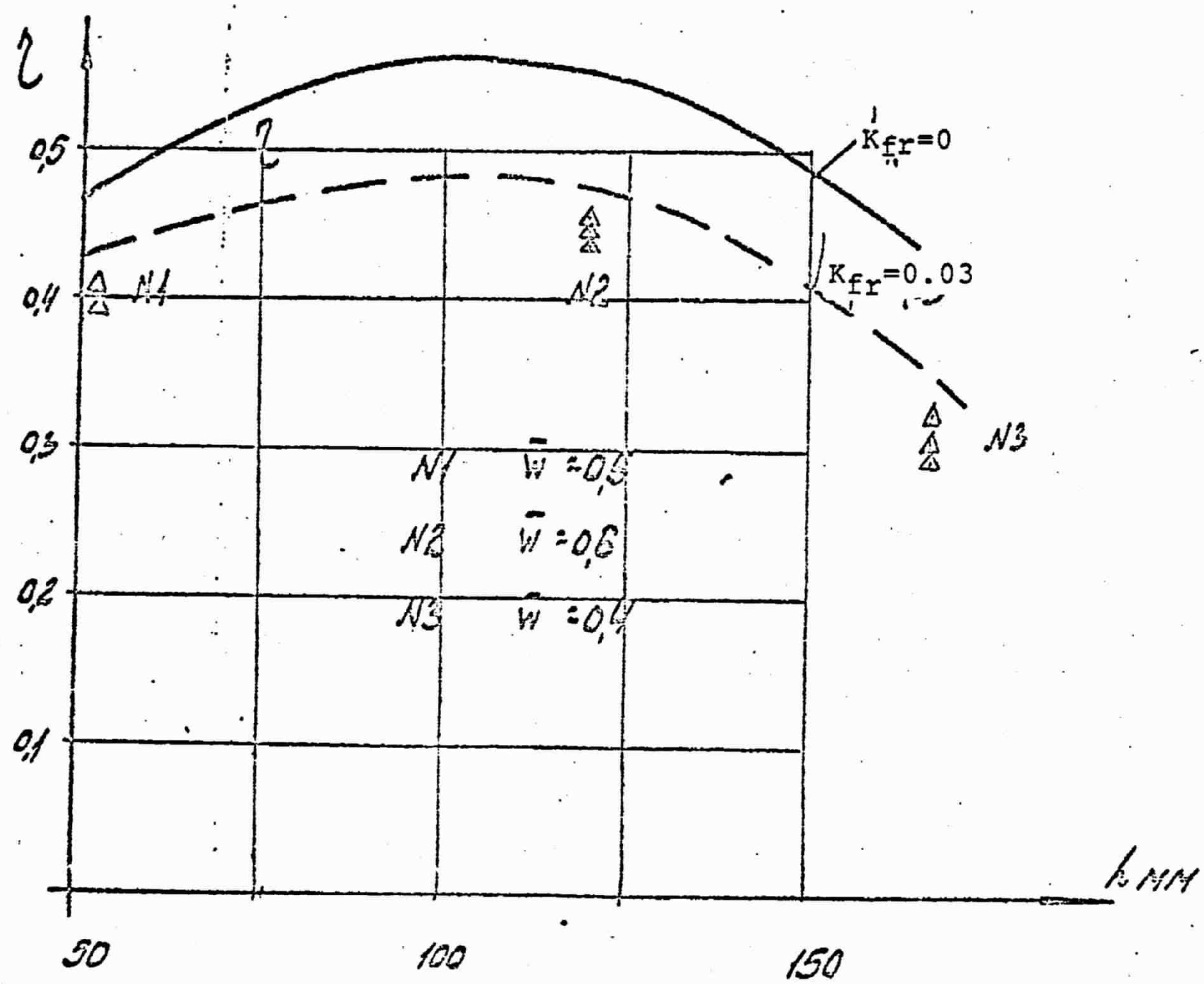

Фиг. 5. Зависимость КПД сопел от длины и параметра $\bar{W}$.

— расчет без учета трения $\lambda_{тр.} = 0$.

– – расчет с учетом трения $\lambda_{тр} = 0{,}03$.

Δ экспериментальные точки.

Fig. 5. The dependence of the efficiency of the nozzle on length and the parameter W.

—— computed without consideration for friction $K_{fr}=0$

– – computed with consideration for friction $K_{fr}=0.003$.

Δ experimental points.

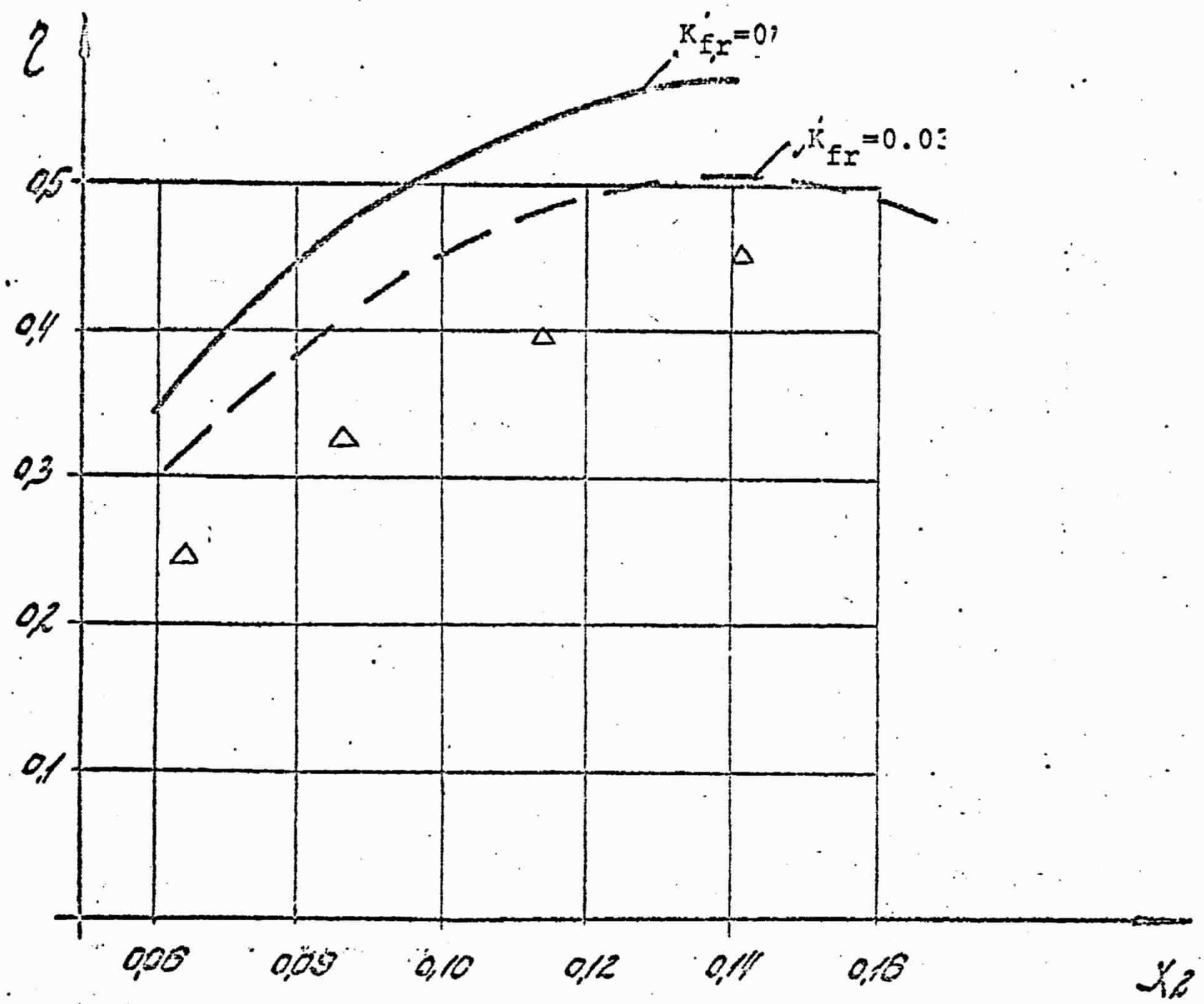

Фиг. 6. Зависимость КПД сопла от степени сухости парожидкостной смеси на выходе из сопла.

—— расчёт без учета трения, $\lambda_{тр}=0$.
— — расчёт с учетом трения, $\lambda_{тр}=0{,}03$
△ экспериментальные точки.

Fig. 6. Dependence of nozzle efficiency on the degree of dryness for the vapor-liquid mixture at the nozzle outlet.
_____ computed without consideration of friction $K_{fr}=0$
_ _ _ computed with consideration of the friction $K_{fr}= 0.03$

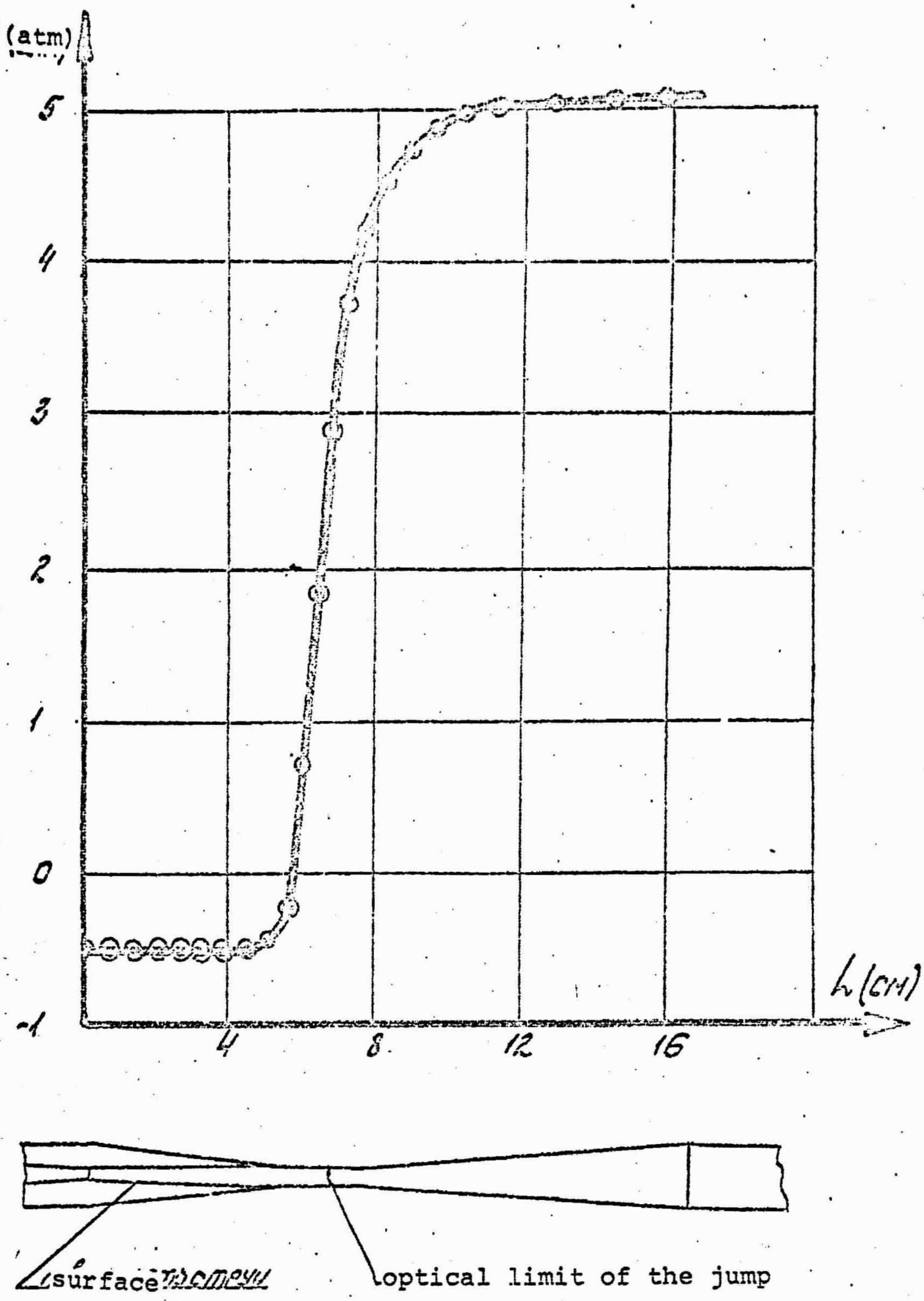

Фиг. 7.

Распределение давления по длине камеры смещения (профиль 2-4С).

Fig. 7. Distribution of pressure along the length of the mixture chamber (profile 2-4 C)

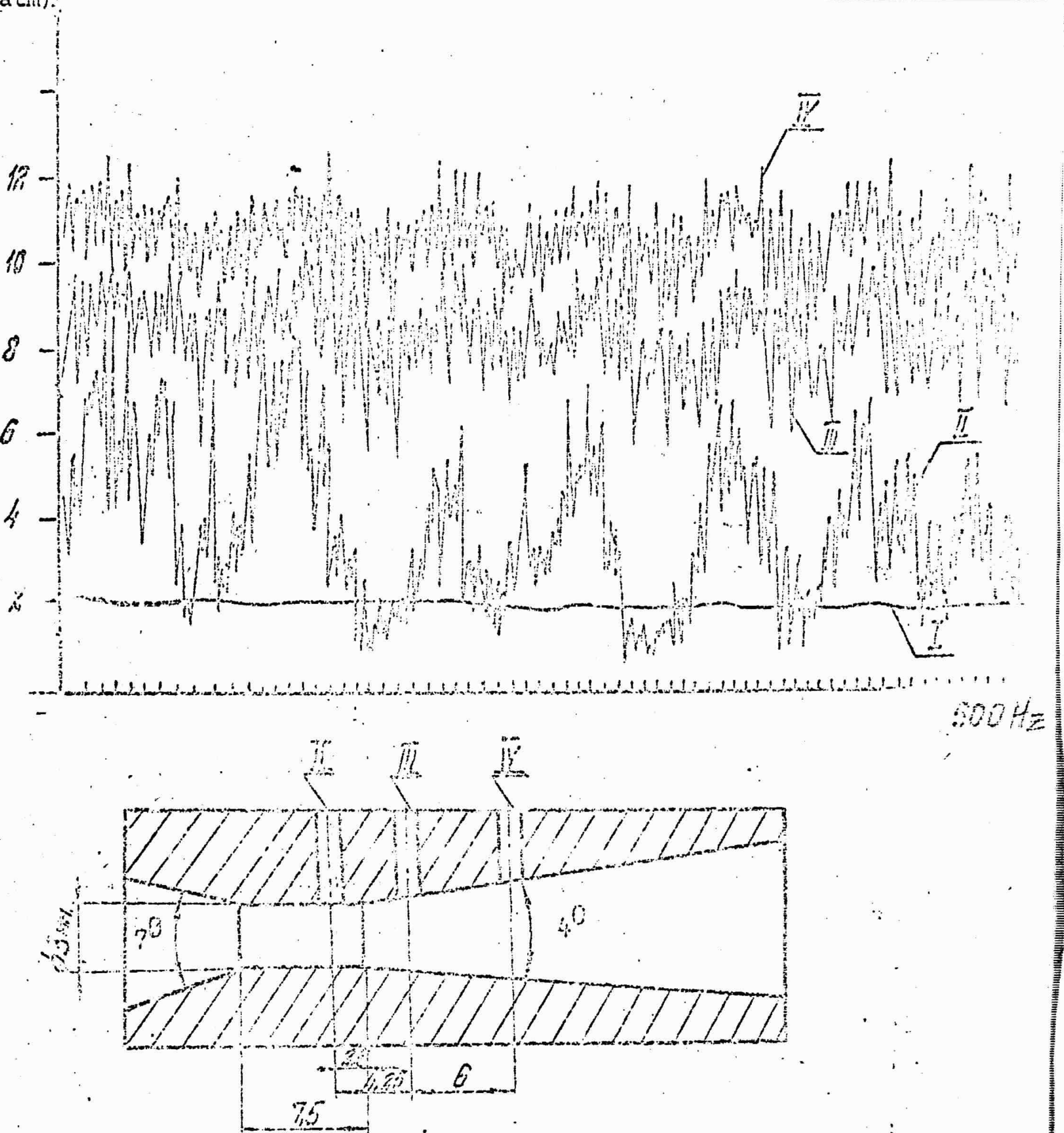

$G=0.295$ kg/sec
$P_{m.c.}=0.33$ atm

I Pressure of the vapor at inlet на вход
II, III, IV } Pressure af the jump

Фиг. 8. Осциллограмма скачка

Fig. 8. Oscillogram of the jump.

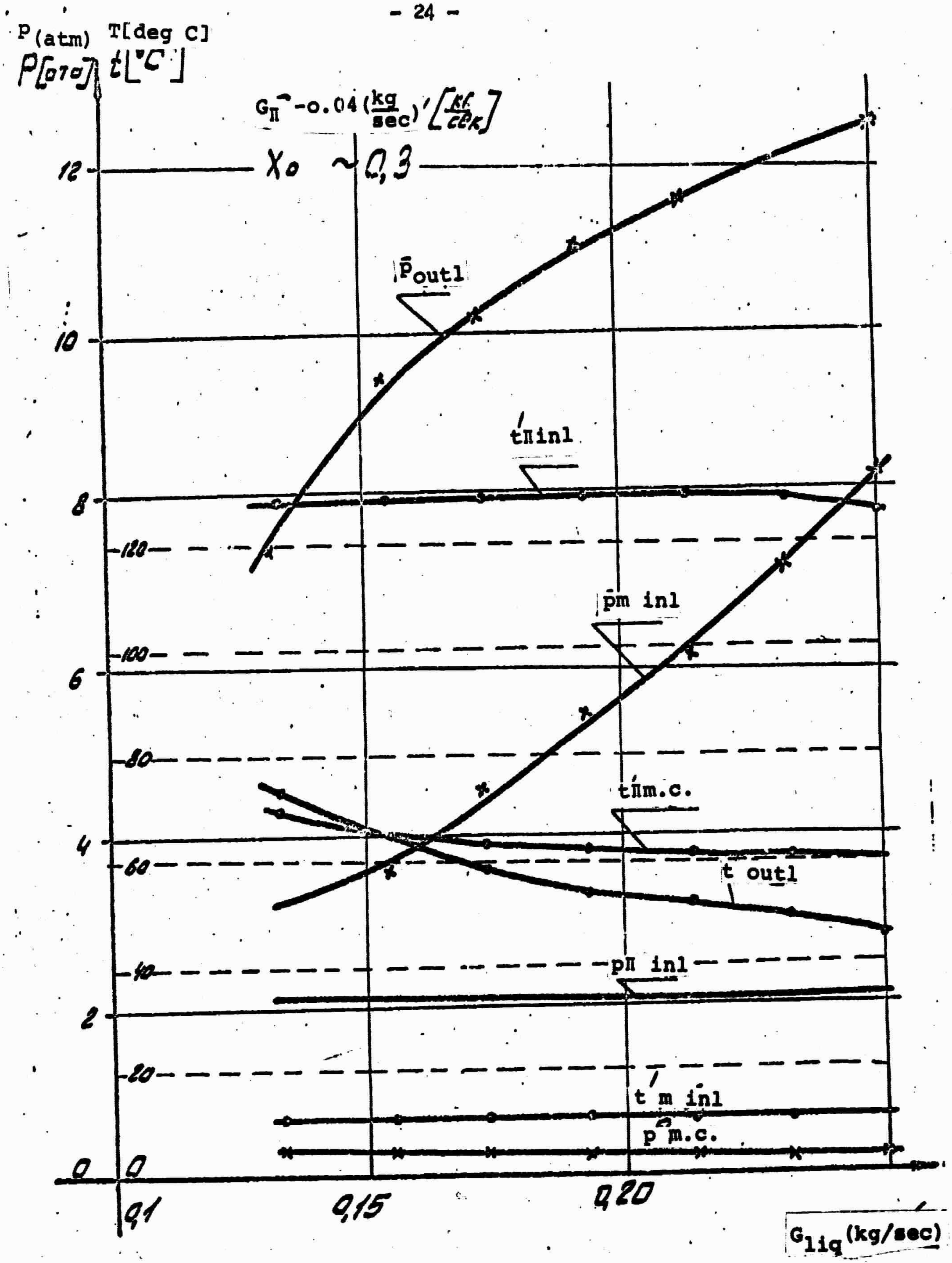

ФИГ. 9. ВНЕШНИЕ ХАРАКТЕРИСТИКИ РАЗГОННОГО УСТРОЙСТВА.

Fig. 9. Outside characteristics of the accelerator.

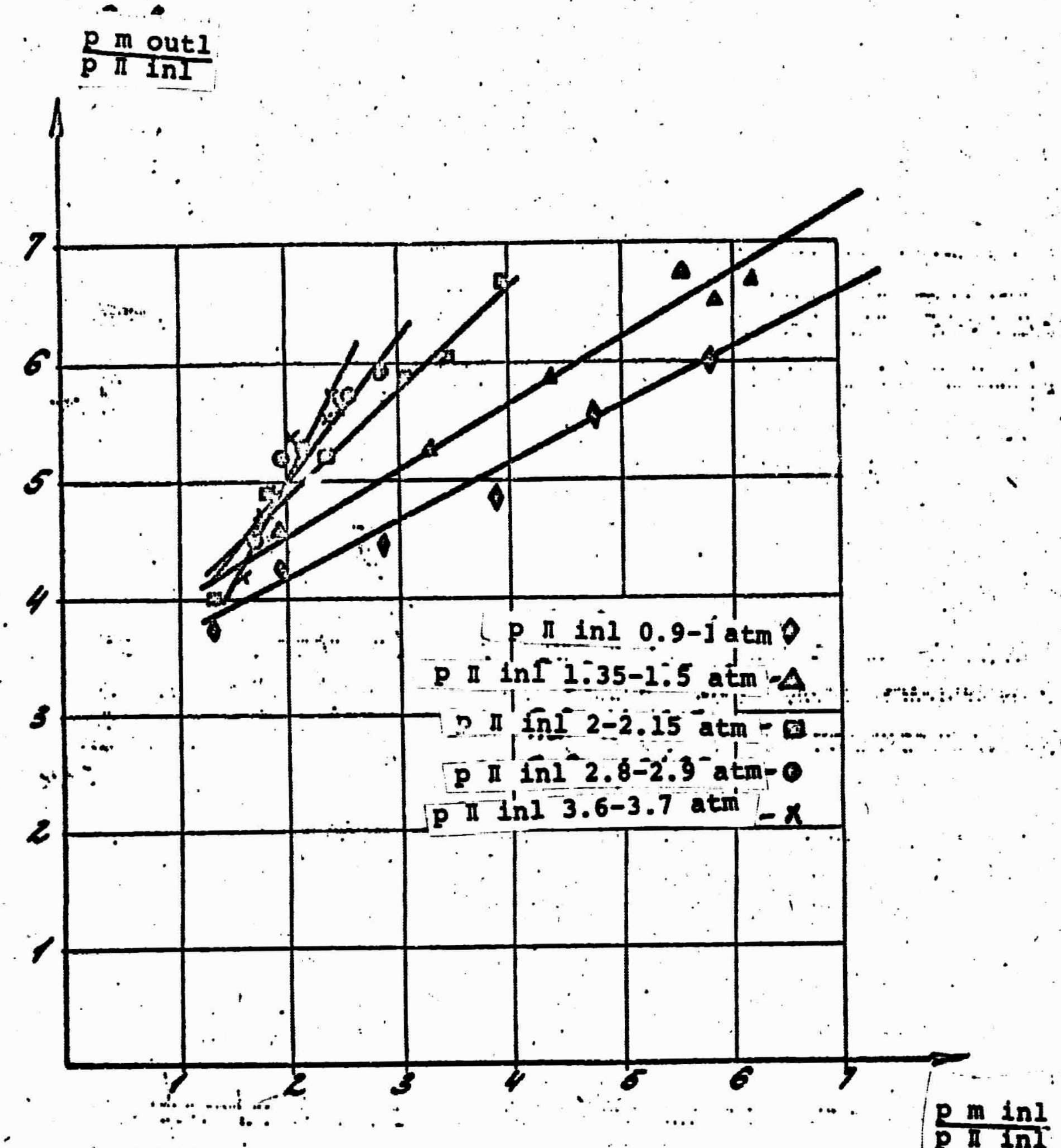

Фиг. 10. Давление на выходе из РУ при различных давлениях пара и жидкости на входе.

Fig. 10. Pressure at the outlet of the accelerator at various pressures for vapor and liquid at the entrance.

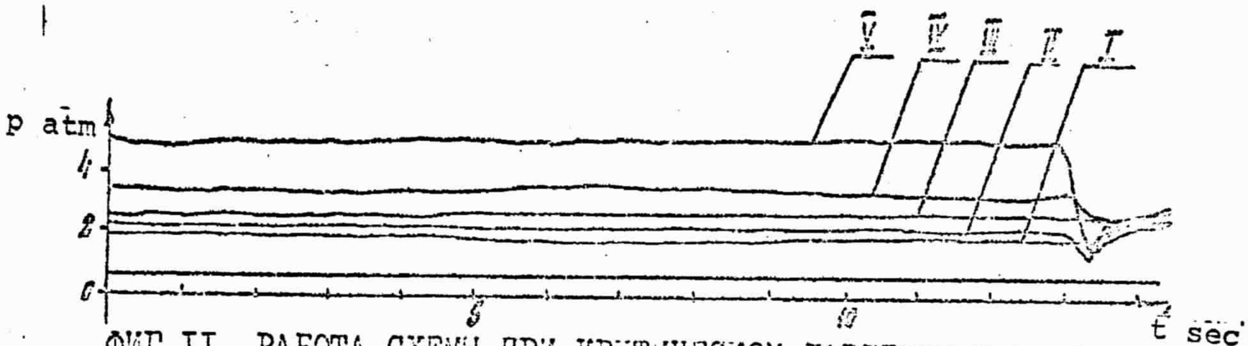

ФИГ.II. РАБОТА СХЕМЫ ПРИ КРИТИЧЕСКОМ ДАВЛЕНИИ В РАСШ

Fig. 11. Operation of the scheme during critical pressure in the expansion tank.

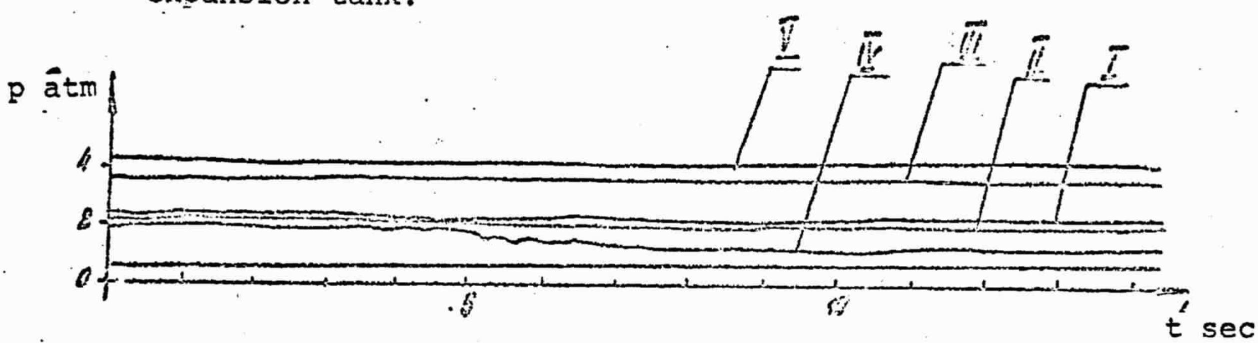

ФИГ.I2. УВЕЛИЧЕНИЕ ТЕПЛОВОЙ МОЩНОСТИ НА 20% НОМИНАЛЬНОЙ.

Fig. 12. Increase of thermal power by 20% of nominal.

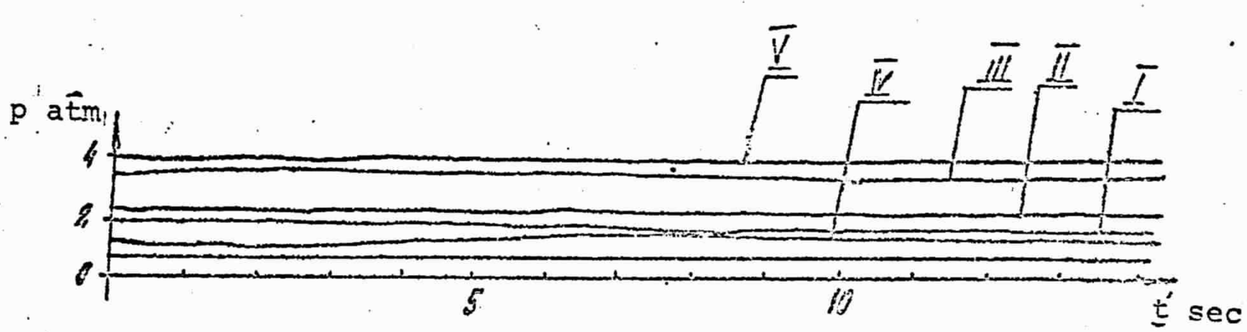

ФИГ.I3. УМЕНЬШЕНИЕ ТЕПЛОВОЙ МОЩНОСТИ НА 20% НОМИНАЛЬНОЙ.

Fig. 13. Decrease of thermal power by 20% of nominal.